

Exploring incomplete fusion fraction in $^{6,7}\text{Li}$ induced nuclear reactions

V. V. Parkar^{1,*}, V. Jha¹, and S. Kailas^{1,2}

¹Nuclear Physics Division, Bhabha Atomic Research Centre, Mumbai - 400085, India

²UM-DAE Centre for Excellence in Basic Sciences, Mumbai - 400098, India

Abstract. We have included breakup effects explicitly to simultaneously calculate the measured cross-sections of the complete fusion, incomplete fusion, and total fusion for $^{6,7}\text{Li}$ projectiles on various targets using the Continuum Discretized Coupled Channels method. The breakup absorption cross-sections obtained with different choices of short range imaginary potentials are utilized to evaluate the individual α -capture and d/t-capture cross-sections and compare with the measured data. It is interesting to note, while in case of ^7Li projectile the cross-sections for triton-ICF/triton-capture is far more dominant than α -ICF/ α -capture at all energies, similar behavior is not observed in case of ^6Li projectile for the deuteron-ICF/deuteron-capture and α -ICF/ α -capture. Both these observations are also corroborated by the experimental data for all the systems studied.

1 Introduction

In recent years, there is a lot of data available for complete fusion (CF) cross-sections with $^{6,7}\text{Li}$ and ^9Be projectiles on various targets [1–13]. The measured complete fusion cross-sections are found to be suppressed compared to the Coupled Channel calculations or One Dimensional barrier penetration model calculations at above barrier energies. It is also observed that the suppression factor is independent of target atomic number and it increases with decreasing the breakup threshold of the projectile; *viz.*, for ^6Li ($S_{\alpha-d}=1.47$ MeV), the suppression factor is $\sim 32\%$ and for ^7Li ($S_{\alpha-t}=2.47$ MeV), it is $\sim 26\%$ [3]. The origin of this suppression is still not known properly. It is possible that the fraction lost in CF can be directly attributed to incomplete fusion (ICF) fraction, where only part of the projectile fuses with the target. However, ICF can also accommodate the processes where there is a transfer of one nucleon to/from the projectile, which then breaks and subsequent absorption in the target. There are recent studies by Canberra, Australia group [14–16] on measurement of life times and the breakup probabilities of $^{6,7}\text{Li}$ and ^9Be nuclei on various targets. From their studies they have concluded that the prompt breakup/near target breakup is partially responsible for the suppression in CF.

In the experiments involving light targets, it is difficult to distinguish residues from CF and ICF channels as both can give rise to the same residual nucleus. Hence in that mass region, the measured cross-sections are denoted as total fusion (TF). In the medium and heavy mass targets, it is possible to distinguish between residues from CF and ICF, hence simultaneous measurement of CF, ICF and TF can be possible. The two major methods of on-line and offline gamma ray measurements are generally

adopted for extraction of these residue cross-sections and hence CF and ICF cross-sections. In few studies where the residues are alpha active, *viz.*, in the case of $^{6,7}\text{Li}+^{209}\text{Bi}$ and $^9\text{Be}+^{208}\text{Pb}$ [2], the CF and ICF cross-sections were extracted from offline alpha counting.

In this proceedings, we report some of the interesting observations from the ICF cross-sections with $^{6,7}\text{Li}$ projectiles, which is described in Section 2. We have also performed coupled channels calculations using short range imaginary potential for simultaneous explanation of CF, ICF and TF cross-sections, which is described in Section 3. The summary and future outlook of the present work is given in Section 4.

2 Interesting observations from the literature on the ICF data with $^{6,7}\text{Li}$ projectiles

Although, there is a lot of data available for CF cross-sections with $^{6,7}\text{Li}$ projectiles on various targets, only limited data is available for ICF channel with these projectiles. We have used the available ICF cross-section data for $^{6,7}\text{Li}+^{209}\text{Bi}$ [2], $^7\text{Li}+^{198}\text{Pt}$ [17], $^{6,7}\text{Li}+^{197}\text{Au}$ [18] and $^7\text{Li}+^{159}\text{Tb}$ [19] reactions and discussed some of the striking features. In Fig. 1, experimental t-ICF and α -ICF cross-section data as a function of $E_{c.m.}/V_B$ for (a) $^7\text{Li}+^{209}\text{Bi}$ [2], (b) $^7\text{Li}+^{198}\text{Pt}$ [17], (c) $^7\text{Li}+^{197}\text{Au}$ [18], and (d) $^7\text{Li}+^{159}\text{Tb}$ [19] reactions are compared and shown with filled circle and filled diamond symbols, respectively. It is evident from this figure that t-ICF cross-sections are much more dominant compared to ones for α -ICF cross-sections at all the measured energies with ^7Li projectile. Intuitively, we expect this behavior as triton while approaching the target sees lower Coulomb barrier compared to alpha particle approaching the target, hence the cross-

*e-mail: parkarvivek@gmail.com

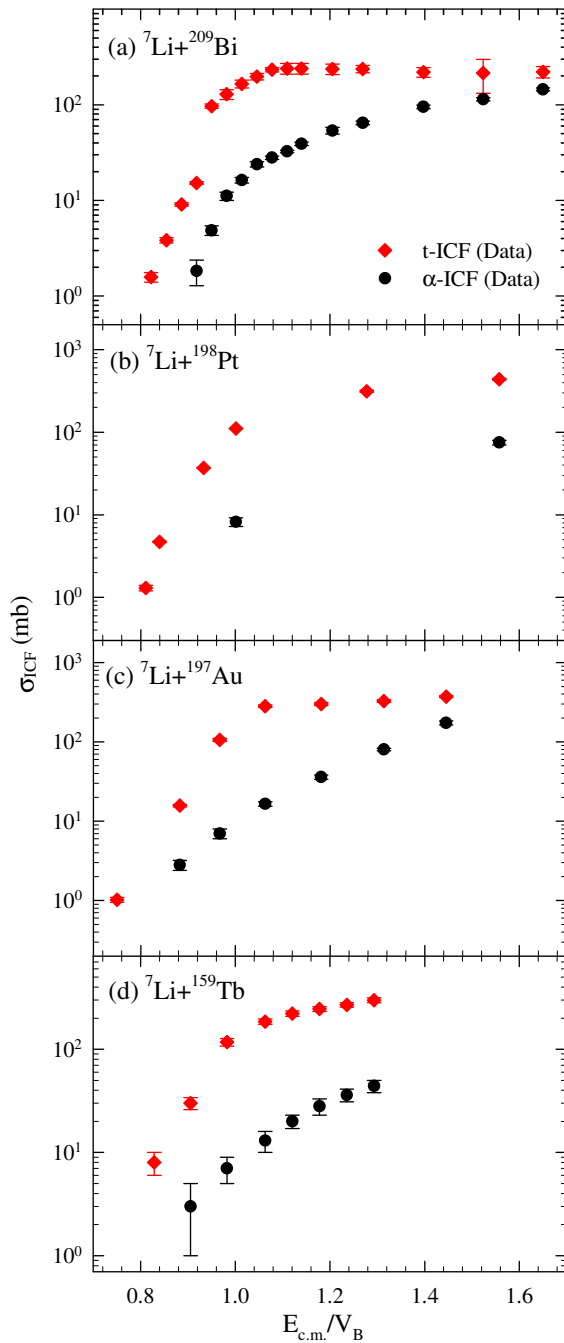


Figure 1. Experimental t-ICF and α -ICF cross-section data as a function of $E_{c.m.}/V_B$ for (a) ${}^7\text{Li}+{}^{209}\text{Bi}$ [2], (b) ${}^7\text{Li}+{}^{198}\text{Pt}$ [17], (c) ${}^7\text{Li}+{}^{197}\text{Au}$ [18], and (d) ${}^7\text{Li}+{}^{159}\text{Tb}$ [19] reactions are compared with filled circle and filled diamond symbols, respectively. It is evident from the figure that t-ICF is dominant compared to α -ICF at all the measured energies.

section for t-ICF is more compared to ones for α -ICF. It is to be noted that deuteron and proton pickups in the target would give the same ERs as those following t-ICF process and subsequent few neutron evaporation. Hence, from experiments it is difficult to separate these three processes.

In Fig. 2, experimental d-ICF and α -ICF cross-section data as a function of $E_{c.m.}/V_B$ for (a) ${}^6\text{Li}+{}^{209}\text{Bi}$ [2], and (b) ${}^6\text{Li}+{}^{197}\text{Au}$ [18] reactions are compared and shown with

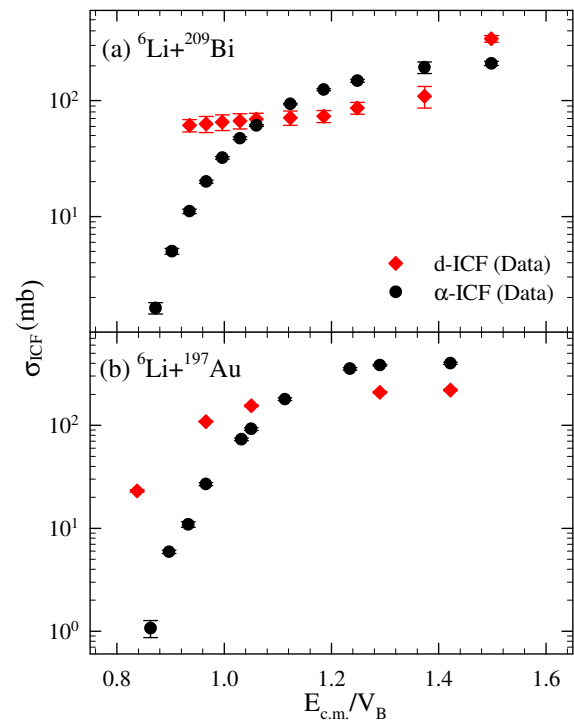


Figure 2. Experimental d-ICF and α -ICF cross-section data as a function of $E_{c.m.}/V_B$ for (a) ${}^6\text{Li}+{}^{209}\text{Bi}$ [2], and (b) ${}^6\text{Li}+{}^{197}\text{Au}$ [18] reactions are compared with filled circle and filled diamond symbols, respectively. It is evident that d-ICF dominates over α -ICF, but at above barrier energies α -ICF and d-ICF are of similar order.

filled circle and filled diamond symbols, respectively. From this figure, it is seen that around barrier energies, d-ICF dominates over α -ICF, but at above barrier energies α -ICF and d-ICF are of similar order. At above barrier energies, deuteron breaks into proton and neutron and subsequent escape of neutron can be one of the possible reasons for lower cross-section in d-ICF. More data are required with d-ICF and α -ICF with several targets to comment on this behavior.

3 Coupled Channels calculations for simultaneous description of CF, ICF and TF data

Recently, we have reported the method for simultaneous description of CF, ICF and TF data for the ${}^6,{}^7\text{Li}+{}^{209}\text{Bi}$ and ${}^6,{}^7\text{Li}+{}^{198}\text{Pt}$ reactions [20] using Continuum Discretized Coupled Channel (CDCC) calculations involving short range imaginary potential. The details of the calculation method are given in that paper and only short summary is given here. In this paper, we have shown the similar calculations for estimation of CF, ICF and TF cross-sections in ${}^7\text{Li}+{}^{197}\text{Au}$ reaction. The calculations were performed using the code FRESKO version FRESKO 2.9 [21]. The coupling scheme used in CDCC is similar to that described in our earlier works [22]. In ${}^7\text{Li}$, couplings were included to the $1/2^-$ first excited state, the $5/2^-$ and $7/2^-$ resonances

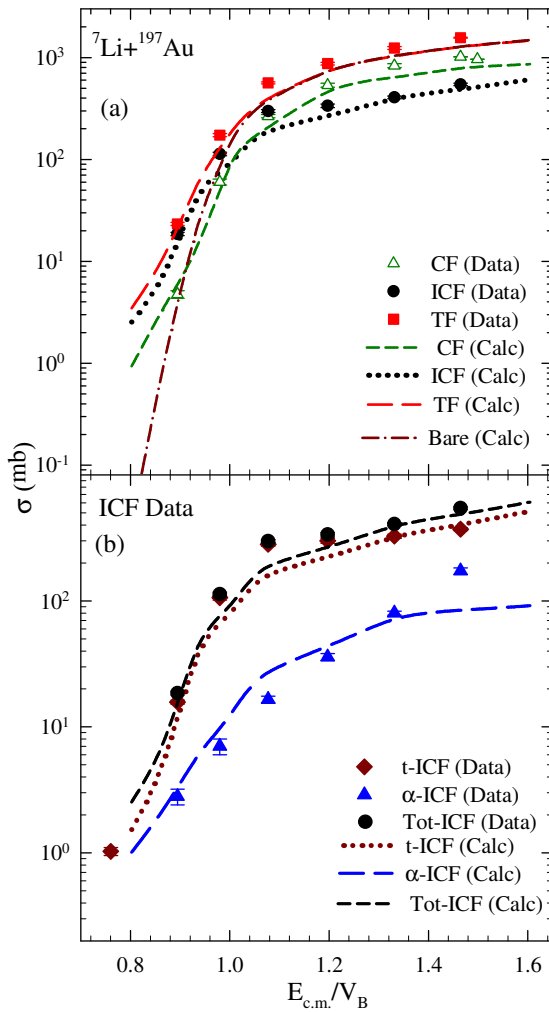


Figure 3. (a) The data of Complete Fusion (CF), Incomplete Fusion (ICF) and Total fusion (TF)=CF+ICF for ${}^7\text{Li}+{}^{197}\text{Au}$ reaction from Ref. [18] are compared with the calculations. (b) Comparison of individual ICF contributions from α -ICF, t-ICF along with Tot-ICF with the calculations. (see text for details).

and the $L = 0, 1, 2, 3$ α -t continuum. The binding potentials for α -t in ${}^7\text{Li}$ are taken from Ref.[23].

In the CDCC calculations, the fusion cross sections can be obtained as the total absorption cross section, which is equal to the difference of the total reaction cross section σ_R and the cross section σ_D of all explicitly coupled direct reaction channels. The required fragment-target potentials were generated in the cluster folding (CF) model using real potentials, *viz.*, $V_{\alpha-T}$ taken as Sao-Paulo potential [24], while V_{d-T} and V_{t-T} were taken from Refs. [25] and [26], respectively. In the calculations presented here, TF cross-sections were first calculated by including the short-range imaginary (W_{SR}) volume type potentials in the coordinates of both projectile fragments relative to the target, as in Ref. [27], whereas ICF cross-sections were calculated with short range imaginary potentials for only one fragment relative to the target. The fusion cross-section is calculated in terms of that amount of flux which leaves the coupled

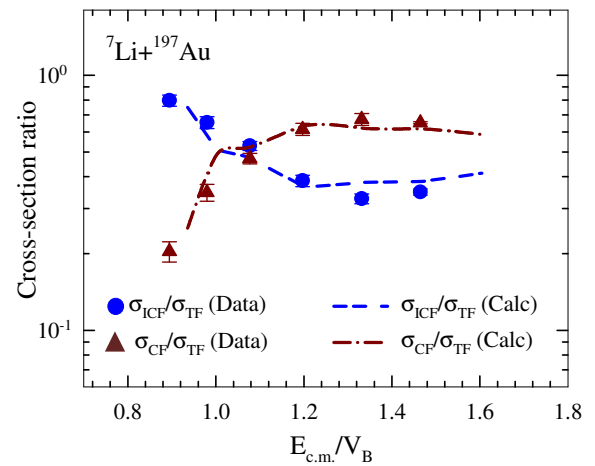


Figure 4. The ratio of cross-section, $\sigma_{\text{ICF}}/\sigma_{\text{TF}}$ and $\sigma_{\text{CF}}/\sigma_{\text{TF}}$ derived from the calculations as a function of $E_{\text{c.m.}}/V_B$ for ${}^7\text{Li}+{}^{197}\text{Au}$ reaction are shown by dashed and dashed-dot lines, respectively. The symbols denote the experimental data (see text for details).

channels set (total absorption cross-section) because of the short-range imaginary part of the optical potential used for the fragment-target potentials. The use of this short-range imaginary potential is equivalent to the use of an incoming boundary condition inside the Coulomb barrier.

In Fig. 3(a) results of the calculations for the TF, CF and ICF cross-sections are shown with long dashed, short dashed and dotted lines, respectively along with the experimental data for ${}^7\text{Li}+{}^{197}\text{Au}$ reaction. The bare calculations (without breakup couplings) were also performed and the calculated fusion cross-sections are denoted by dashed-dot-dot lines in the above mentioned figure. It is seen that at energies above the Coulomb barrier, the calculations which include the couplings and calculations that omit them have negligible difference, but at energies below the barrier, the coupled TF cross-sections are enhanced in comparison to bare TF cross-sections. The breakup of the projectile nucleus can take place (i) spontaneously in the nuclear or Coulomb field of the target or (ii) it may be triggered by the transfer processes. The latter process is found to be important in some recent works [15, 16] which could explain partially the CF suppression. We have considered the breakup absorption taking place only via the first route in our calculations. To describe the experimental ICF data, the breakup absorption has been calculated with a modified value of imaginary radius parameter and thus it effectively models the full breakup absorption.

The corresponding individual ICF cross-sections, $\sigma_{\alpha\text{-ICF}}$ and $\sigma_{\text{t-ICF}}$, are extracted and shown in Fig. 3(b). The long dashed, dotted and short dashed lines denote the α -ICF, t-ICF and Tot-ICF calculations, respectively. From the figure, it is evident that the t-ICF is dominant than α -ICF and almost equal to the Total ICF cross-section.

The ratio of cross-sections, $\sigma_{\text{ICF}}/\sigma_{\text{TF}}$ and $\sigma_{\text{CF}}/\sigma_{\text{TF}}$ derived from the calculations as a function of $E_{\text{c.m.}}/V_B$ for ${}^7\text{Li}+{}^{197}\text{Au}$ reaction are shown by dashed and dashed-dot

lines in Fig. 4, respectively. The corresponding experimental data of $\sigma_{\text{ICF}}/\sigma_{\text{TF}}$ and $\sigma_{\text{CF}}/\sigma_{\text{TF}}$ are shown with filled circle and filled triangle in Fig. 4, respectively. From the figure it is evident that (i) Ratios of $\sigma_{\text{ICF}}/\sigma_{\text{TF}}$ and $\sigma_{\text{CF}}/\sigma_{\text{TF}}$ remain approximately constant over the energy range above the Coulomb barrier. (ii) For energies below the barrier, the $\sigma_{\text{ICF}}/\sigma_{\text{TF}}$ ratio increase while $\sigma_{\text{CF}}/\sigma_{\text{TF}}$ ratio decrease. This shows the dominance of ICF at below barrier energies in TF over CF cross-sections. The $\sigma_{\text{ICF}}/\sigma_{\text{TF}}$ ratio at above barrier energies gives the value of suppression factor in CF, which is found to be in agreement ($\sim 30\%$) with the literature data with ${}^7\text{Li}$ projectiles from various measurements [3]. Similar observation was also indicated in ${}^{6,7}\text{Li}+{}^{209}\text{Bi}$ and ${}^{6,7}\text{Li}+{}^{198}\text{Pt}$ reactions [20].

4 Summary and Futute Outlook

In summary, from the available experimental data, we have highlighted the differences in individual ICF cross-sections for ${}^6\text{Li}$ and ${}^7\text{Li}$ projectiles on various targets. The individual ICF cross-sections imply that the d-ICF cross-section is of similar order that of α -ICF cross-section in case of ${}^6\text{Li}$, while t-ICF cross-section is much more than α -ICF cross-section in case of ${}^7\text{Li}$. More data of d-ICF, α -ICF and t-ICF simultaneously for various systems are required to further emphasize this observation.

We have performed Continuum Discretized Coupled Channel calculations using cluster folding potentials in the real part along with short-range imaginary part for calculation of CF, ICF and TF cross-sections for ${}^7\text{Li}+{}^{197}\text{Au}$ reaction. The simultaneous explanation of the measured experimental data for the CF, ICF and TF cross-sections over the entire energy range is obtained using calculations in the full quantum mechanical approach. The calculated ICF fraction which is the ratio of ICF and TF as a function of energy is found to be constant at energies above the barrier and and it increases at energies below the barrier. This ratio which signifies the suppression of CF in TF is constant at above barrier energies and it is in agreement with the available data for several systems. At below barrier, as the ratio increases, it shows the enhanced importance of ICF contribution in TF at below barrier energies. Similar calculations are in progress to study the systematic

behavior of individual ICF fractions with ${}^{6,7}\text{Li}$ projectiles for different target systems.

References

- [1] L. F. Canto, P. R. S. Gomes, R. Donangelo, J. Lubian, and M. S. Hussein, Phys. Rep. **596**, 1 (2015) and references therein.
- [2] M. Dasgupta *et al.*, Phys. Rev. **C 70**, 024606 (2004).
- [3] V. V. Parkar *et al.*, Phys. Rev. **C 82**, 054601 (2010).
- [4] C. S. Palshetkar *et al.*, Phys. Rev. **C 82**, 044608 (2010).
- [5] Y. D. Fang *et al.*, Phys. Rev. **C 91**, 014608 (2015).
- [6] P. R. S. Gomes *et al.*, Phys. Rev. **C 73**, 064606 (2006).
- [7] H. Kumawat *et al.*, Phys. Rev. **C 86**, 024607 (2012).
- [8] P. K. Rath *et al.*, Nucl. Phys. **A 874**, 14 (2012).
- [9] P. K. Rath *et al.*, Phys. Rev. **C 79**, 051601R (2009).
- [10] M. K. Pradhan *et al.*, Phys. Rev. **C 83**, 064606 (2011).
- [11] A. Mukherjee *et al.*, Phys. Letts. **B 636**, 91 (2006).
- [12] S. P. Hu *et al.*, Phys. Rev. **C 91**, 044619 (2015).
- [13] Y. W. Wu *et al.*, Phys. Rev. **C 68**, 044605 (2003).
- [14] D. H. Luong *et al.*, Phys. Rev. **C 88**, 034609 (2013).
- [15] Sunil Kalkal *et al.*, Phys. Rev. **C 93**, 044605 (2016).
- [16] K. J. Cook *et al.*, Phys. Rev. **C 93**, 064604 (2016).
- [17] A. Shrivastava *et al.*, Phys. Lett. **B 718**, 931 (2013).
- [18] C. S. Palshetkar *et al.*, Phys. Rev. **C 89**, 024607 (2014).
- [19] R. Broda *et al.*, Nucl. Phys. **A 248**, 356 (1975).
- [20] V. V. Parkar, V. Jha and S. Kailas, Phys. Rev. **C 94**, 024609 (2016).
- [21] I. J. Thompson, Comput. Phys. Rep. **7**, 167 (1988).
- [22] V. Jha and S. Kailas, Phys. Rev. **C 80**, 034607 (2009).
- [23] B. Buck and A. C. Merchant, J. Phys. G: Nucl. Part. Phys. **14**, L211 (1988).
- [24] L. C. Chamon *et al.*, Phys. Rev. **C 66**, 014610 (2002).
- [25] W. W. Daehnick, J. D. Childs, and Z. Vrcelj, Phys. Rev. **C 21**, 2253 (1980).
- [26] F. D. Becchetti and G. W. Greenlees, Phys. Rev. **182**, 1190 (1969).
- [27] A. Diaz-Torres, I. J. Thompson, and C. Beck, Phys. Rev. **C 68**, 044607 (2003).